Cancer Imaging

RESEARCH ARTICLE Open Access

Prospective evaluation of Gadoxetate-enhanced magnetic resonance imaging and computed tomography for hepatocellular carcinoma detection and transplant eligibility assessment with explant histopathology correlation

Kartik S. Jhaveri[1*], Ali Babaei Jandaghi[2], Rajesh Bhayana[3], Khaled Y. Elbanna[3], Osvaldo Espin-Garcia[4,5], Sandra E. Fischer[6], Anand Ghanekar[7] and Gonzalo Sapisochin[7]

Abstract

Background We aimed to prospectively compare the diagnostic performance of gadoxetic acid-enhanced MRI (EOB-MRI) and contrast-enhanced Computed Tomography (CECT) for hepatocellular carcinoma (HCC) detection and liver transplant (LT) eligibility assessment in cirrhotic patients with explant histopathology correlation.

Methods In this prospective, single-institution ethics-approved study, 101 cirrhotic patients were enrolled consecutively from the pre-LT clinic with written informed consent. Patients underwent CECT and EOB-MRI alternately every 3 months until LT or study exclusion. Two blinded radiologists independently scored hepatic lesions on CECT and EOB-MRI utilizing the liver imaging reporting and data system (LI-RADS) version 2018. Liver explant histopathology was the reference standard. Pre-LT eligibility accuracies with EOB-MRI and CECT as per Milan criteria (MC) were assessed in reference to post-LT explant histopathology. Lesion-level and patient-level statistical analyses were performed.

Results Sixty patients (49 men; age 33–72 years) underwent LT successfully. One hundred four non-treated HCC and 42 viable HCC in previously treated HCC were identified at explant histopathology. For LR-4/5 category lesions, EOB-MRI had a higher pooled sensitivity (86.7% versus 75.3%, $p < 0.001$) but lower specificity (84.6% versus 100%, $p < 0.001$) compared to CECT. EOB-MRI had a sensitivity twice that of CECT (65.9% versus 32.2%, $p < 0.001$) when all HCC identified at explant histopathology were included in the analysis instead of imaging visible lesions only. Disregarding the hepatobiliary phase resulted in a significant drop in EOB-MRI performance (86.7 to 72.8%, $p < 0.001$). EOB-MRI had significantly lower pooled sensitivity and specificity versus CECT in the LR5 category with lesion size < 2 cm (50% versus 79%, $p = 0.002$ and 88.9% versus 100%, $p = 0.002$). EOB-MRI had higher sensitivity (84.8% versus 75%, $p < 0.037$) compared to CECT for detecting < 2 cm viable HCC in treated lesions. Accuracies of LT eligibility assessment were comparable between EOB-MRI (90–91.7%, $p = 0.156$) and CECT (90–95%, $p = 0.158$).

*Correspondence:
Kartik S. Jhaveri
kartik.jhaveri@uhn.ca
Full list of author information is available at the end of the article

Conclusion EOB-MRI had superior sensitivity for HCC detection; however, with lower specificity compared to CECT in LR4/5 category lesions while it was inferior to CECT in the LR5 category under 2 cm. The accuracy for LT eligibility assessment based on MC was not significantly different between EOB-MRI and CECT.

Trial registration ClinicalTrials.gov Identifier: NCT03342677, Registered: November 17, 2017.

Keywords Carcinoma, Hepatocellular, Liver transplantation, Contrast media, Magnetic resonance imaging, Tomography, Computed, Gadoxetic acid, Milan criteria

Key points

- Gadoxetic acid-enhanced Liver MRI had better diagnostic performance in some categories compared to Computed Tomography for the diagnosis of Hepatocellular carcinoma in patients with liver cirrhosis enlisted for transplantation.
- Gadoxetic acid-enhanced liver MRI had a significantly superior 'real world' or true sensitivity for hepatocellular carcinoma diagnosis versus computed tomography.
- Liver transplantation eligibility assessment was not significantly different between gadoxetic acid-enhanced liver MRI and computed tomography.

Background

Liver transplantation (LT) is the treatment of choice for patients with hepatocellular carcinoma (HCC) confined to the liver who are not eligible for partial hepatic resection or ablation, while palliative therapies such as transarterial chemoembolization (TACE), radiotherapy, and systemic agents are recommended for those with more advanced disease [1]. According to EASL guidelines, LT is also recommended for patients with very early-stage HCC [2].

Preoperative imaging is relied upon not only for HCC detection but also for the determination of LT eligibility [3]. While different LT jurisdictions around the world employ slightly different criteria to determine LT eligibility, all rely upon diagnostic imaging studies to provide critical information about HCC size, number, and presence of macrovascular invasion to determine waitlist priority for LT candidates. For example, in the United States, LT candidates are required to have CECT or MRI every 3 months while awaiting transplantation to determine that their HCC burden falls within the Milan Criteria (MC); those who do not exceed MC receive additional MELD exception points until they undergo LT, while those who are found to exceed MC may be delisted [4]. Since awaiting LT can result in HCC progression, the Organ Procurement and Transplantation Network (OPTN)/United Network for Organ Sharing (UNOS) has developed a supplemental system for prioritization of patients with HCC meeting OPTN T2 criteria (a single HCC of 2–5 cm or three or fewer HCCs 1–3 cm) for LT and a downstaging protocol using locoregional therapies for those exceeding MC [5].

To date, limited studies have prospectively compared the diagnostic performance of CECT and MRI for detection of HCC in LT candidates [6–9], with no consensus on which of CECT, extracellular gadolinium-based contrast-enhanced MRI (EC-MRI), or MRI with hepatobiliary agents is superior [10]. CECT can be performed quickly and is more widely available compared to MRI but has lower contrast resolution with incremental radiation exposure [11]. Gadoxetate-enhanced Liver MRI (EOB-MRI) has had variable results compared to EC-MRI [12] and CECT depending on HCC size and diagnostic criteria utilized in LT candidates, with only a few studies utilizing liver explants as the reference standard [13, 14]. Notably, the lack of whole-liver explant correlation and retrospective evaluations have also probably overestimated imaging sensitivity for HCC diagnosis [15–17].

Thus, we aimed to prospectively compare the diagnostic performance of EOB-MRI and CECT for HCC detection and transplant eligibility in pre-LT cirrhotic patients with explant histopathology correlation.

Methods

Study participants

This was a prospective, single-institution HIPAA compliant, and ethics-approved study. Between November 2017 and April 2021, written informed consent was obtained from consecutive patients following chart review in a pre-transplant clinic. Inclusion criteria were: (a) liver cirrhosis enlisted for LT with a high probability of undergoing transplantation within 12 months, and (b) diagnosed, suspected and or treated HCC with priority MELD points based on cancer diagnosis. The exclusion criteria were patient age < 18 years, low Glomerular filtration rate (GFR) (< 30 mL/min/1.73 m2), high bilirubin (> 3 mg/dl), pregnancy, MRI contraindications (pacemaker etc.), prior systemic HCC treatment, bridging therapies (TACE or ablation) between imaging and LT or removal from the LT waiting list. Patients underwent CECT and EOB-MRI

alternately every 3 months until LT. Among 101 enrolled patients, the final cohort comprised 60 patients with exclusion of 41 patients (Fig. 1 and Table 1).

Imaging techniques

CECT was performed on either of two scanners (Aquilion ONE or Aquilion 64, Toshiba CA, USA;) with a standardized multiphasic liver protocol (Additional file 1). EOB-MRI was performed on a 1.5 T (Magnetom Avanto; Siemens Healthcare, Erlangen, Germany) or 3 T (Magnetom Verio with Tim system; Siemens Health care, Erlangen, Germany) MRI scanner with multichannel phased array coils (16 or 32 channels) using a standardized liver protocol (Additional file 2).

Image evaluation

While patients were enrolled, and imaging scans were performed prospectively, EOB-MRI and CECT performed closest to LT were retrieved and de-identified for retrospective image evaluation from departmental PACS. Two abdominal radiologists independently reviewed CECT and EOB-MRI data with a gap of at least 4 weeks to minimize recall bias. They were blinded to the explant histopathology findings but knew that the patients were cirrhotic with or without prior interventional therapy and enlisted for LT.

Non-treated lesions

Using LI-RADS v2018, each reader assessed the presence or absence of major and ancillary imaging features for all non-treated hepatic lesions measuring $\geq$ 0.5 cm on EOB-MRI (Additional file 3) and CECT. Lesion characteristics recorded on EOB-MRI and CECT are summarized in Additional files 4 and 5. Subtraction images were reviewed to evaluate arterial phase hyperenhancement (APHE). Washout and capsule enhancement were determined on portal venous or additionally on equilibrium phase (CECT) [18]. The largest axial diameter was measured in portal venous or hepatobiliary phase and, if invisible on the sequence with best margin demarcation. Threshold growth was not included in the assessment as no prior imaging studies were included for analysis. LI-RADS score was assigned to each recorded lesion. Analyses were performed considering HCC diagnosis as an observation score of LR-4/5 and LR-5 alone.

Treated lesions

All treated lesions were evaluated based on the LI-RADS treatment response algorithm (TRA), and a LI-RADS treatment response (LR-TR) category was assigned as viable, nonviable, equivocal or nonevaluable (Additional file 6) [18].

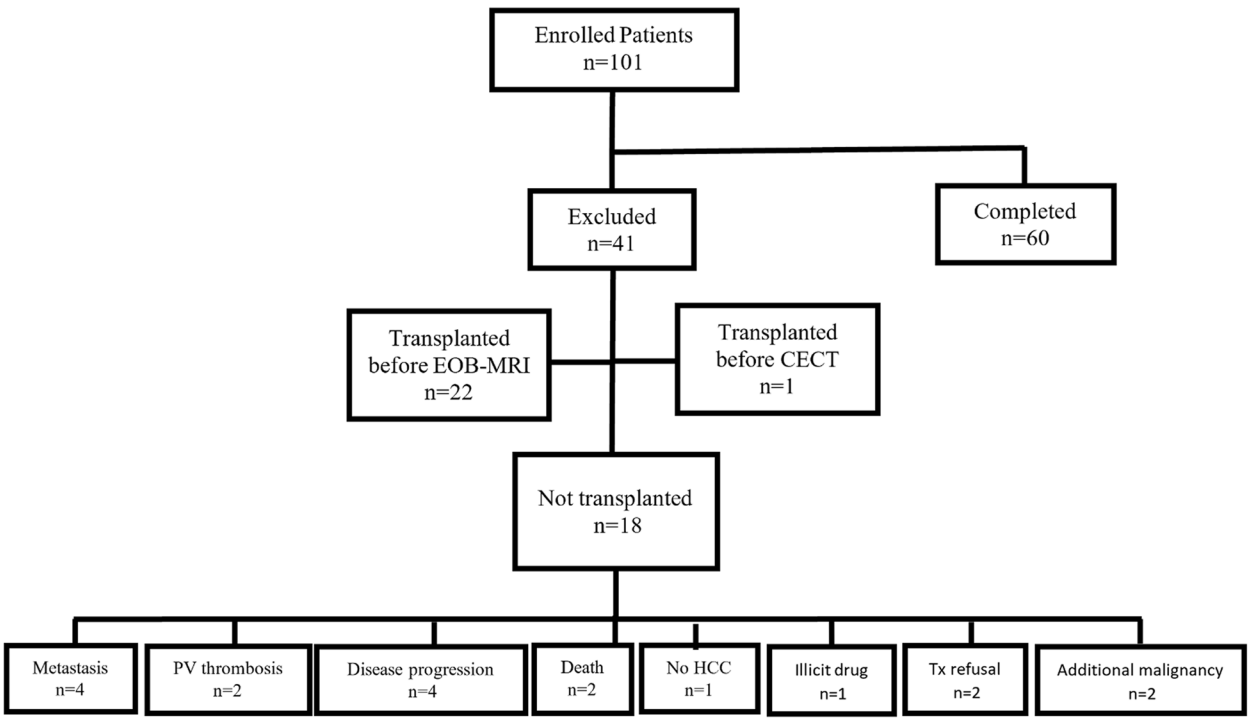

Fig. 1 Patient enrollment flowchart. Abbreviations: EOB-MRI: Gadoxetic acid-enhanced MRI, CECT: Contrast-enhanced Computed Tomography, PV: portal vein, HCC: hepatocellular carcinoma, Tx: transplantation

Table 1 Patient demographic and clinical characteristics

All patients	60
Characteristic	
Mean age at surgery (range, years)	62.5 ± 7.5 (33–72)
Sex	
Male	49 (81.7)
Female	11 (18.3)
Cause of chronic liver disease	
HCV	20 (33.3)
HBV	16 (26.7)
Alcohol	11 (18.3)
NASH	9 (15)
Other	4 (6.7)
LRT (per patient)	46 (76.7)
Type of LRT (per lesion)	
Total number of treated observations	134 (100)
RFA	78 (58.2)
TACE	15 (11.2)
TACE and RFA	29 (21.7)
BE	4 (3)
MWA	3 (2.2)
SBRT	1 (0.7)
Not specified	4 (3)
Type of liver transplantation	
Living donor	5 (8.3)
Deceased donor	55 (91.7)
Time interval (day)	Mean (SD), Median (range)
CT and EOB-MRI	90.3 (41.4), 84.5 (0.0–271.0)
CT and LT	100.7 (63.9), 101.5 (0.0–279.0)
EOB-MRI and LT	69.1 (49.7), 61 (3–192)
Last imaging and LT	39.8 (28.9), 35 (0–110)

Data in parentheses are numbers used to calculate the percentages

BE bland embolization, *LRT* local-regional therapy, *MWA* microwave ablation, *RFA* radiofrequency ablation, *SBRT* stereotactic body radiation therapy, *TACE* transarterial chemoembolization

Reference standard

A liver pathologist with more than 15 years of experience examined all the liver explants. The explanted livers were routinely sectioned into 5-mm-thick axial slices, and all suspicious macroscopic, bulging, or discolored nodules at gross examination underwent histopathological evaluation. The pathology report included final diagnosis, tumor size and segment location, degree of tumor differentiation, presence of microvascular or macrovascular invasion, presence of capsule, degree of necrosis, and maximum size of viable tumor in treated observations. Tumor stage was reported according to the 8th edition staging system of the American Joint Committee on Cancer (AJCC) [19]. Complete pathologic necrosis (CPN) (100%) in treated observations was used as a reference standard for nonviable tumors, and non-CPN (< 100%) was used for viable HCC.

Radiology-pathology correlation

A study investigator (ABJ) correlated the recorded observations on EOB-MRI and CECT with those on explant pathology reports based on lesion size and segment location. Lesions were matched if the difference between the pathologically and radiologically measured sizes was less than 10 mm, and no similar-sized lesion was observed in the same segment. Cholangiocarcinoma and mixed HCC-cholangiocarcinoma tumors were analyzed as non-HCC tumors. HCCs detected only on histopathology without corresponding LR-4 or 5 imaging observations in the same segment location were regarded as false-negative (FN), and the contrary was defined as false-positive (FP).

Transplant allocation

Prospective LT allocation was determined as per Extended Toronto criteria (ETC), which offers LT irrespective of HCC size or number but requires no macrovascular invasion, extrahepatic disease, systemic cancer-related symptoms, or poorly differentiated tumors [20]. Thus, we evaluated simulated LT eligibility as per MC (single HCC ≤ 5 cm or 3 or fewer HCCs ≤3 cm, no vascular invasion and extrahepatic disease) [21] by each reader with EOB-MRI and CECT utilizing LI-RADS and OPTN criteria, verified in reference to explant histopathology. Regarding the OPTN criteria, all lesions detected on imaging were classified according to the OPTN classification system based on size and enhancement patterns (Additional file 7) [5]. In patients with treated observations (class 5T), the diameter of viable tumors was considered for determining LT eligibility. Therefore, patients having a single lesion (non-treated, class 5B; or treated, class 5T) with a maximum diameter of at least 2 cm and less than or equal to 5 cm, and those with up to 3 lesions (non-treated and/or treated), each greater than or equal to 1 cm and less than or equal to 3 cm (i.e., lesions in class 5A, class 5B only if less than 3 cm and class 5T only if greater than or equal to 1 cm and less than or equal to 3 cm) were considered eligible for LT.

Statistical analysis

The diagnostic performance of EOB-MRI and CECT was compared for each reader based on a lesion-by-lesion level analysis of histopathologically confirmed HCC. Two lesion level analyses were performed: (i) wherein only the imaging detected lesions matched with corresponding histopathology correlation were included and (ii) wherein all lesions detected on histopathology irrespective of imaging visibility were included with the HCCs not

detected on imaging being categorized as false negatives (FN). A p-value <0.05 was considered statistically significant. Interobserver agreement was assessed via concordance rate (%) of diagnosis between the readers for EOB-MRI and CT. Reader-level scores were compared using McNemar tests. The sensitivity and corresponding 95% confidence intervals (CIs) of EOB-MRI and CECT in detecting HCC in correlation with the reference standard in pooled-reader analyses using a generalized estimating equations approach as previously described were calculated [22]. The performance of CECT and EOB-MRI on simulated LT allocation as per MC based on LI-RADS and OPTN criteria was also evaluated.

Results

Histopathologic results

One hundred seventeen non-treated liver lesions (mean size: 1.3 ± 0.65 cm, range: 0.5–3.5 cm) and 134 (mean size: 2.1 ± 1.32 cm, range: 0.1–6.0 cm) treated observations were recorded in 60 liver explants. Table 2 demonstrates the histopathologic findings of all non-treated lesions and treated observations. The distribution of non-treated HCCs and viable HCCs is shown in Additional file 8.

Diagnostic performance of CECT and EOB-MRI for HCC detection

Observations with corresponding histopathologic abnormality (Table 3)

Non-treated lesions

LR-4/5 score as HCC

Without size consideration, HCC detection sensitivity and accuracy were higher for both readers with EOB-MRI versus CECT. The pooled sensitivity was significantly greater with EOB-MRI (Fig. 2), while the pooled specificity was significantly lower with EOB-MRI versus CECT. For lesions < 2 cm, EOB-MRI had higher sensitivity and accuracy for both readers and only for one reader in the ≥2 cm group. EOB-MRI had higher pooled sensitivities for both < 2 cm and ≥ 2 cm lesions and a lower pooled specificity for the < 2 cm group, although without reaching statistical significance.

LR-5 score as HCC

Regardless of size, the sensitivity and accuracy were higher with CECT compared to EOB-MRI for both readers. However, pooled sensitivity with CECT was

Table 2 Histopathologic characteristics of liver lesions at explant pathology

	Non-treated lesions				
	HCC	cHCC-CCA	CCA	Benign	Total
Number of lesions (%)	104 (88.9)	2 (1.7)	1 (0.9)	10 (8.5)	117 (100)
Mean size ± SD (range, cm)	1.3 ± 0.63 (0.5–3.5)	1.5 (0.5–2.5)	1.0 (NA)	1.3 ± 0.8 (0.6–32)	1.3 ± 0.65 (0.5–3.5)
Number in subgroups (%)					
0.5–0.9 cm	34 (29.1)	1 (0.9)	–	4 (3.4)	39 (33.3)
1–1.9 cm	56 (47.8)	–	1 (0.9)	4 (3.4)	61 (52.1)
≥ 2 cm	14 (12)	1 (0.9)	–	2 (1.7)	17 (14.6)
Differentiation (%)					
Well	9 (7.7)	–	–	–	9 (7.7)
Moderately	92 (78.6)	1 (0.9)	1 (0.9)	–	94 (80.3)
poorly	3 (2.6)	1 (0.9)	–	–	4 (3.4)
	Treated observations				
	Viable HCC	Viable cHCC-CCA		Non-viable HCC	Total
Number of lesions (%)	42 (31.3)	2 (1.5)		90 (67.2)	134 (100)
Whole mean size ± SD (range, cm)	2.9 ± 2.0 (0.6–10.5)	3.0 (2.0–4.0)		2.4 ± 1.3 (0.2–6.0)	2.6 ± 1.6 (0.2–10.5)
Viable mean size ± SD (range, cm)	1.6 ± 1.3 (0.1–5.5)	1.1 (0.5–1.6)		0 ± 0	1.5 ± 1.2 (0.1–5.5)
Number in subgroups (%)					
< 2 cm	32 (23.9)	2 (1.5)		36 (26.8)	70 (52.2)
≥ 2 cm	10 (7.5)	–		54 (40.3)	64 (47.8)
Differentiation states (%)					
Well	4 (3)	–		–	4 (3)
Moderately	36 (26.8)	–		–	36 (26.8)
poorly	2 (1.5)	2 (1.5)		–	4 (3)

HCC hepatocellular carcinoma, *cHCC-CCA* combined hepatocellular-cholangiocarcinoma, *CCA* cholangiocarcinoma, *SD* standard deviation

Table 3 Diagnostic performance of CECT and EOB-MRI observations with corresponding histopathologic abnormality

LR-4 or 5 score as HCC													
Size		**CECT**					**EOB-MRI**					*p*-value	
		Se	Sp	NPV	PPV	Acc	Se	Sp	NPV	PPV	Acc	Se	Sp
overall	R1	80.9 (38/47)	100 (4/4)	30.8 (4/13)	100 (38/38)	82.4 (42/51)	96.3 (78/81)	85.7 (6/7)	66.7 (6/9)	98.7 (78/79)	95.5 (84/88)		
	R2	69 (29/42)	100 (4/4)	23.5 (4/17)	100 (29/29)	71.7 (33/46)	76.6 (59/77)	83.3 (5/6)	21.7 (5/23)	98.3 (59/60)	77.1 (64/83)		
	Pooled	75.3	100				86.7	84.6				< 0.001	< 0.001
< 2 cm	R1	81 (34/42)	100 (2/2)	20 (2/10)	100 (34/34)	81.8 (36/44)	95.4 (62/65)	80 (4/5)	57.1 (4/7)	98.4 (62/63)	94.3 (66/70)		
	R2	64.9 (24/37)	100 (2/2)	13.3 (2/15)	100 (24/24)	66.7 26/39)	73.4 (47/64)	75 (3/4)	15 (3/20)	97.9 (47/48)	73.5 (50/68)		
	Pooled	73.4	100				84.5	77.8				1	1
≥ 2 cm	R1	80 (4/5)	100 (2/2)	66.7 (2/3)	100 (4/4)	85.7 (6/7)	100 (16/16)	100 (2/2)	100 (2/2)	100 (16/16)	100 (18/18)		
	R2	100 (5/5)	100 (2/2)	100 (2/2)	100 (5/5)	100 (7/7)	92.3 (12/13)	100 (2/2)	66.7 (2/3)	100 (12/12)	93.3 (14/15)		
	Pooled	90	100				96.6	100				0.452	0.452
LR-5 score as HCC													
size		**CECT**					**EOB-MRI**					*p*-value	
		Se	Sp	NPV	PPV	Acc	Se	Sp	NPV	PPV	Acc	Se	Sp
overall	R1	86.5 (32/37)	100 (4/4)	44.4 (4/9)	100 (32/32)	87.8 (36/41)	54.2 (32/59)	100 (7/7)	20.6 (7/34)	100 (32/32)	59.1 (39/66)		
	R2	68.6 (24/35)	100 (4/4)	26.7 (4/15)	100 (24/24)	71.8 (28/39)	50 (30/30)	83.3 (5/6)	14.3 (5/35)	96.8 (30/31)	53 (35/66)		
	Pooled	77.8	100				52.1	92.3				0.243	0.243
1–1.9 cm	R1	87.5 (28/32)	100 (2/2)	33.3 (2/6)	100 (28/28)	88.2 (30/34)	48.8 (21/43)	100 (5/5)	18.5 (5/27)	100 (21/21)	54.2 (26/48)		
	R2	70 (21/30)	100 (2/2)	18.2 (2/11)	100 (21/21)	71.9 (23/32)	51.1 (24/47)	75 (3/4)	11.5 (3/26)	96 (24/25)	52.9 (27/51)		
	Pooled	79	100				50	88.9				0.002	0.002
≥ 2 cm	R1	80 (4/5)	100 (2/2)	66.7 2/3)	100 (4/4)	85.7 (6/7)	68.8 (11/16)	100 2/2)	28.6 (2/7)	100 (11/11)	72.2 (13/18)		
	R2	60 (3/5)	100 (2/2)	50 (2/4)	100 (3/3)	71.4 (5/7)	46.2 (6/13)	100 (2/2)	22.2 (2/9)	100 (6/6)	53.3 8/15)		
	Pooled	70	100				58.6	100				1	1

Data are percentages, with numerators and denominators in parentheses

Acc accuracy, *CECT* contrast-enhanced computed tomography, *EOB-MRI* Gadoxetic acid-enhanced MRI, *NPV* negative predictive value, *PPV* positive predictive value, *R1* reader 1, *R2* reader 2, *Se* sensitivity, *Sp* specificity

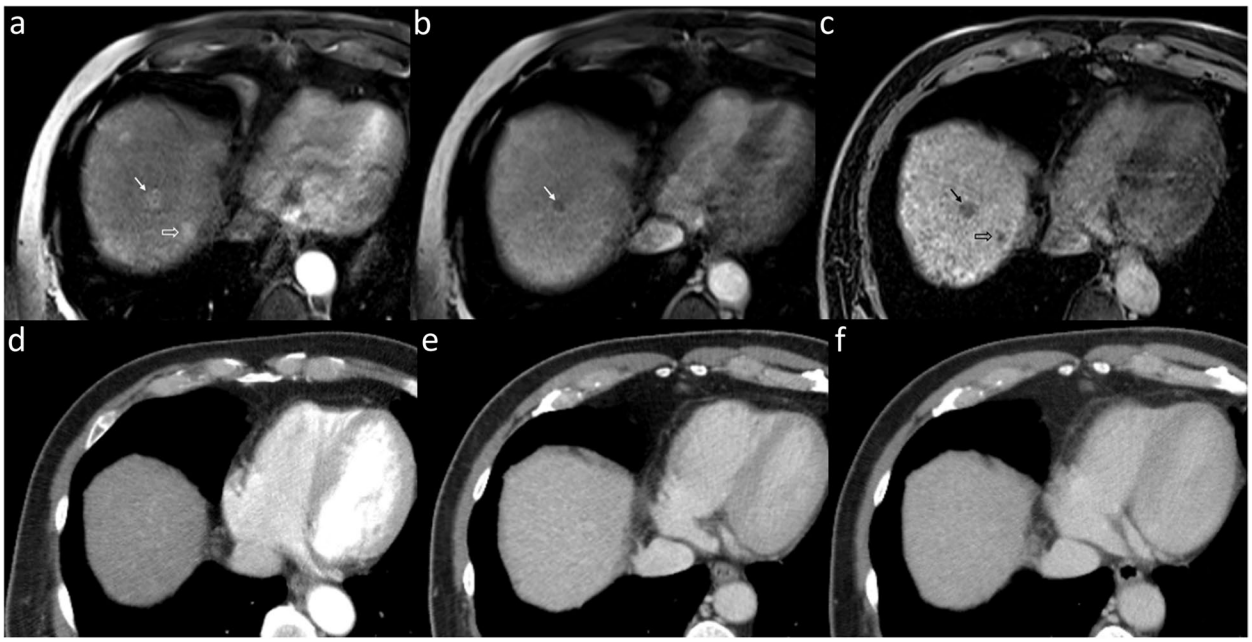

Fig. 2 Superiority of EOB-MRI compared to CECT in detecting HCC. In a 68-year-old male, EOB-MRI shows a 10-mm arterial phase hyperenhancing HCC (arrow, **a**) in segment 8 with nonperipheral washout (arrow, **b**) and obvious hypointensity on HBP (arrow, **c**) in keeping with LR5. However, the lesion was invisible on all phases of CECT (**d**-**f**). An additional 8-mm arterial hyperenhancing lesion is seen adjacent to the inferior vena cava (hollow arrow, **a**) without venous washout. Considering HBP hypointensity (hollow arrow, **c**), it was categorized as LR-4. Again, the lesion was invisible on CECT. Histopathologic examination of liver explant confirmed HCC at both these locations. Abbreviations: CECT: contrast-enhanced computed tomography, EOB-MRI: Gadoxetate-enhanced-MRI, HCC: hepatocellular carcinoma, HBP: hepatobiliary phase

not-significantly higher than EOB-MRI. The pooled specificity of CECT was again not-significantly greater than EOB-MRI. For HCC size of 1–1.9 cm, a statistically significant lower pooled sensitivity was observed for EOB-MRI vs CECT with a statistically significant higher pooled specificity with CECT. For HCC ≥ 2 cm, the pooled sensitivities were not significantly different, and specificities were equivalent.

LR-3 score

All LR-3 lesions scored by both readers on EOB-MRI and CECT proved to be HCCs at explant histopathology, hence were considered false negative in our analysis. Reader 1 scored fewer LR-3 lesions on EOB-MRI versus CECT (2 vs 8, respectively), with similar occurrences for reader 2 (11 vs 9, respectively). The final diagnosis of LR-2 and LR-3 lesions is summarized in Additional file 9.

Added value of HBP

Irrespective of size, rescoring of observations disregarding HBP as an ancillary LI-RADS feature resulted in a significant drop in pooled sensitivity of LR-4/5 as HCC (86.7 to 72.8%, $p < 0.001$), whereas the specificity remained unchanged (84.6%). The disregard of HBP signal specifically impacted the HCC < 2 cm with a significant drop in pooled sensitivity (84.5 to 69.0%, $p < 0.001$) while specificity (77.8%) remained unchanged (Fig. 3).

Treated observations

Regardless of size, the overall sensitivity, specificity, and accuracy for detection of viable HCC were comparable between readers with EOB-MRI and CECT, with no statistically significant differences in pooled sensitivity and specificity (Table 4). The pooled sensitivity and specificity for detecting viable HCC < 2 cm were significantly greater with EOB-MRI versus CECT (Fig. 4). Further, the pooled sensitivity and specificity for viable HCC ≥ 2 cm were also higher with EOB-MRI versus CECT; however, the differences were statistically insignificant.

'Real-world' (true) sensitivity considering all histopathological proven HCC

Non-treated lesions (Table 5***)***

The 'real-world' or true sensitivity for HCC detection as per LR-4/5 score was significantly superior with EOB-MRI versus CECT for both readers, regardless of HCC size, and the pooled sensitivity of EOB-MRI (65.9%) was more than twice that of CECT (32.2%).

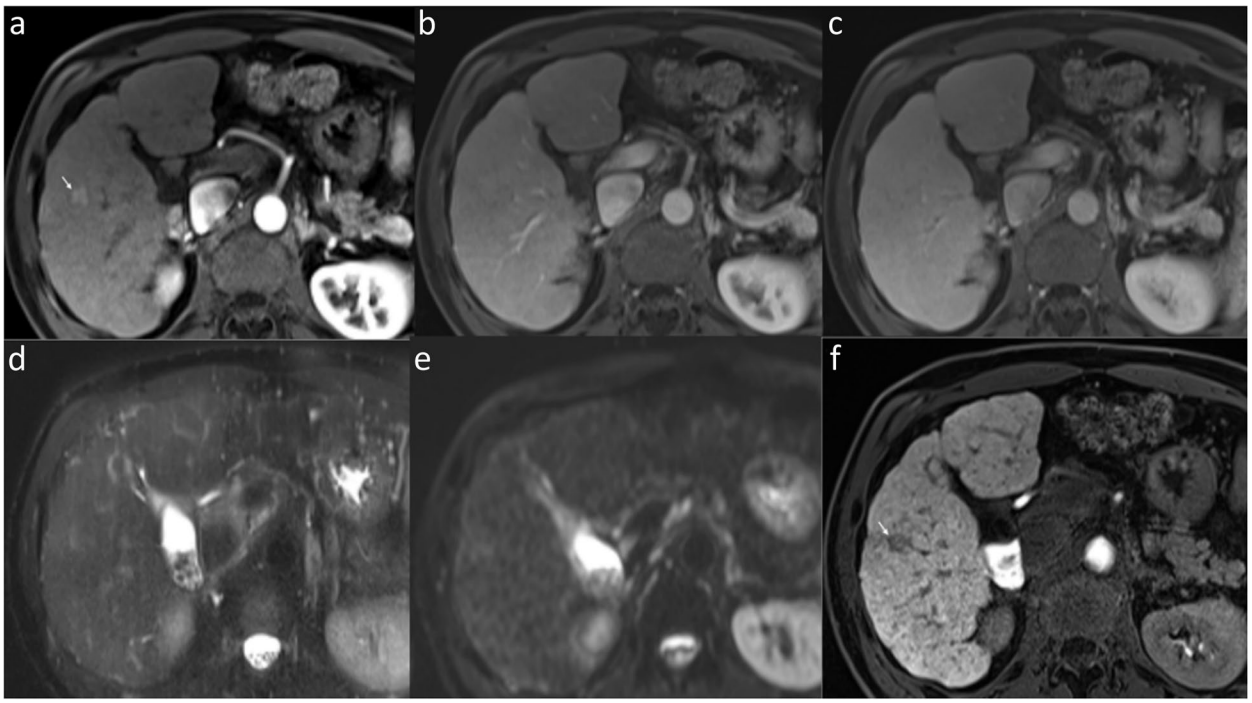

Fig. 3 Impact of HBP on LI-RADS scoring. EOB-MRI in a 53-year-old male shows a 14-mm arterial phase hyperenhancing lesion (arrow, **a**) within segment 5 without washout (**b** and **c**) and without T2 hyperintense signal (**d**) or diffusion restriction (**e**) but with distinct HBP hypointensity (**f**). The LI-RADS score was upgraded to LR-4 based on the HBP signal as an ancillary feature. The lesion was confirmed as HCC at explant histopathology. Abbreviations: CECT: contrast-enhanced computed tomography, EOB-MRI: Gadoxetate-enhanced-MRI, HCC: hepatocellular carcinoma, HBP: hepatobiliary phase, LI-RADS: Liver Imaging Reporting and Data System

Treated observations

Forty-two viable HCCs were identified in 134 treated observations on histopathology. Regardless of size, EOB-MRI had a marginally higher true sensitivity versus CECT utilizing LI-RADS TRA; however, the differences were statistically insignificant.

Simulated LT eligibility

According to explant histopathology findings, 88.3% (53/60) of patients would have been eligible for LT based on MC (Table 6). The overall accuracy in determining LT eligibility using EOB-MRI and CECT was comparable between LI-RADS and OPTN criteria for both readers, and the differences were statistically insignificant (EOB-MRI: $p=0.156$; CT: $p=0.158$). However, both readers showed lower accuracies with CECT and EOB-MRI in detection of patients exceeding versus those meeting MC in reference to histopathology (LI-RADS: $p=0.004$; UNOS guidelines: $p=0.03$). Both readers obtained higher accuracy (with both CECT and EOB-MRI) in predicting patients exceeding MC with HCC diagnosis as per LI-RADS scoring compared to OPTN criteria ($p=0.06$) (Fig. 5).

Interobserver agreement

Interobserver agreement was substantial for EOB-MRI ($\kappa=0.746$, CI 0.635–0.858] and CECT ($\kappa=0.712$; CI: 0.541–0.883) for all observations with a corresponding histopathologic abnormality. CECT had greater interobserver agreement than EOB-MRI for categorizing LR-4/5 ($\kappa=0.572$; CI: 0.219–0.926 vs $\kappa=0.406$; CI: 0.053–0.759). For LR-TR categorization, the interobserver agreement was substantial for EOB-MRI ($\kappa=0.751$, CI: 0.585–0.916) and CECT ($\kappa=0.708$, CI: 0.457–0.958). Interobserver agreement for determination of LT eligibility was moderate for LI-RADS ($\kappa=0.496$ [95% CI, 0.239–0.754] and OTPN criteria ($\kappa=0.565$ [95% CI, 0.209–0.922]).

Discussion

Our study demonstrated that EOB-MRI had an overall superior sensitivity but lower specificity compared to CECT for HCC diagnosis in non-treated LR-4/5 lesions referenced against explant histopathology. EOB-MRI was superior to CECT on analysis by size (< 2 cm versus > 2 cm), although without statistical significance. In the LR-5 category, although EOB-MRI and CECT had statistically similar pooled diagnostic performance without

Table 4 Diagnostic performance of CECT and EOB-MRI for detecting viable HCC with corresponding histopathologic abnormality

Size		CECT					EOB-MRI					*P*-value	
		Se	Sp	NPV	PPV	Acc	Se	Sp	NPV	PPV	Acc	Sen	Sp
overall	R1	58.3 (21/36)	86.6 (58/67)	79.5 (58/73)	70 (21/30)	76.7 (79/103)	66.7 (22/33)	88.5 (54/61)	83.1 (54/65)	75.9 (22/29)	80.9 (76/94)		
	R2	54.5 (18/33)	91.7 (66/72)	81.5 (66/81)	75 (18/24)	80 (84/105)	60 (21/35)	95.8 (69/72)	83.1 (69/83)	87.5 (21/24)	84.1 (90/107)		
	Pooled	56.5	89.2				63.2	92.5				0.312	0.312
< 2 cm	R1	81 (17/21)	50 (9/18)	69.2 (9/13)	65.4 (17/26)	66.7 (26/39)	87.5 (14/16)	50 (7/14)	77.8 (7/9)	66.7 (14/21)	70 (21/30)		
	R2	66.7 (10/15)	75 (12/16)	70.6 12/17)	71.4 10/14)	71 (22/31)	82.4 (14/17)	83.3 (10/12)	76.9 (10/13)	87.5 (14/16)	82.8 (24/29)		
	Pooled	75	61.8				84.8	65.4				0.037	0.037
≥ 2 cm	R1	26.7 (4/15)	100 (49/49)	81.7 (49/60)	100 (4/4)	82.8 (53/64)	47.1 (8/17)	100 (45/45)	83.3 (45/54)	100 (8/8)	85.5 (53/62)		
	R2	44.4 (8/18)	96.4 (54/56)	84.4 54/64)	80 8/10)	83.8 (62/74)	38.9 (7/18)	98.3 (59/60)	84.3 (59/70)	87.5 (7/8)	84.6 (66/78)		
	Pooled	36.4	98.1				42.9	99				0.504	0.504

Data are percentages, with numerators and denominators in parentheses

Acc accuracy, *CECT* contrast-enhanced computed tomography, *EOB-MRI* Gadoxetic acid-enhanced MRI, *NPV* negative predictive value, *PPV* positive predictive value, *R1* reader 1, *R2* reader 2, *Se* sensitivity, *Sp* specificity

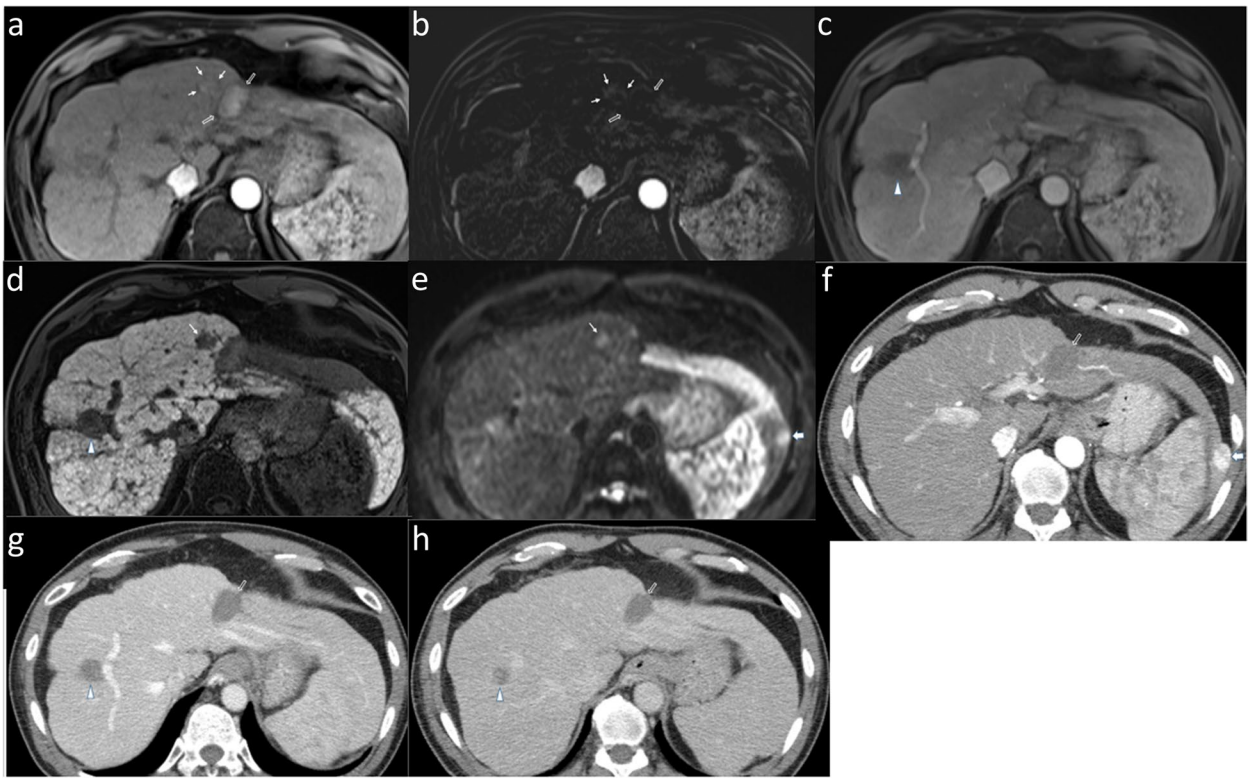

Fig. 4 Superior diagnostic performance of EOB-MRI in detecting < 2 cm-sized viable HCC (LR-TR viable) over CECT. In a 53-year-old man with a history of radiofrequency ablation in segment 3, EOB-MRI (arrows, **a**) demonstrates a 17-mm nodular enhancement which is more conspicuous on the arterial subtraction image (arrows, **b**), anterolateral to the treated observation (hollow arrows, **a** and **b**), without venous phase washout (**c**), but with HBP hypointensity (arrow, **d**) and diffusion restriction (thin arrow, **e**). The treated observation was assigned a viable HCC category on EOB-MRI. On CECT (**f**–**h**), the treated observation (hollow arrow, **f**-**h**) was assigned as non-viable due to lack of nodular arterial phase enhancement. A well-differentiated HCC was detected along the treated observation on histopathologic examination of the liver explant. Additionally demonstrated is a non-enhancing 23-mm treated observation (LR-TR non-viable) in segment 7/8 on EOB-MRI and CECT (arrowheads) with proven complete necrosis on histopathology. As a variant of hepatic morphology, the elongated left liver lobe extends laterally to surround the spleen (beaver tail liver), harboring an 18-mm histopathological proven non-treated HCC (thick arrow, **f**). This lesion manifested typical findings of HCC, including arterial hyperenhancement and washout (LR-5) on both EOB-MRI (not shown) and CECT. Image 5e (thick arrow) depicts the lesion manifesting diffusion restriction. Abbreviations: CECT: contrast-enhanced computed tomography, EOB-MRI: Gadoxetate-enhanced-MRI, HCC: hepatocellular carcinoma, HBP: hepatobiliary phase, LR-TR: Liver Imaging Reporting and Data System-Treatment response

Table 5 Real-world sensitivity of LR-4/5 and viable LR-TR for HCC detection with CECT versus EOB-MRI

LR-4/5 (all HCC ≥ 5 mm at histopathology)				
Size		**CECT**	**EOB-MRI**	*p*-value
Overall	R1	36.5 (38/104)	75 (78/104)	< 0.001
	R2	27.9 (29/104)	56.7 (59/104)	< 0.001
	pooled	32.2 (67/208)	65.9 (137/208)	< 0.001
Treated observations (all viable HCC at histopathology)				
Size		**CECT**	**EOB-MRI**	*p*-value
Overall	R1	47.6 (20/42)	50 (21/42)	1.00
	R2	42.9 (18/42)	50 (21/42)	0.66
	pooled	45.2 (38/84)	50 (42/84)	0.64

Data are percentages, with numerators and denominators in parentheses

CECT contrast-enhanced computed tomography, *EOB-MRI* Gadoxetic acid-enhanced MRI, *R1* reader 1, *R2* reader 2

consideration of HCC size, EOB-MRI was inferior to CECT in the < 2 cm subgroup. HCC detection sensitivity and specificity with CECT and EOB-MRI have wide reported variability in the LR-4/5 and LR-5 categories defined by LI-RADSv2018 [12, 23–25]. A prior meta-analysis of 27 studies concluded that since EOB-MRI showed significantly higher sensitivity and diagnostic accuracy without substantial loss of specificity versus CECT, it should be the preferred imaging modality for small HCC ≤ 2 cm. However, pooling of predominantly retrospective data with heterogeneous inclusion criteria and reference standards may have resulted in overestimated diagnostic performance [17]. Only one retrospective study has utilized liver explants as the sole reference standard comparing CECT versus EOB-MRI for HCC detection based on prior LI-RADS v2017 criteria [13]. They reported superiority of MRI over CECT, without

Table 6 Accuracy of CECT and EOB-MRI for LT eligibility as per Milan criteria with histopathological correlation

	LI-RADS			
	Reader 1		Reader 2	
	CECT	EOB-MRI	CECT	EOB-MRI
Meeting MC	92.5 (49/53)	94.3 (50/53)	98.1 (52/53)	94.3 (50/53)
Exceeding MC	85.7 (6/7)	71.4 (5/7)	71.4 (5/7)	71.4 (5/7)
Overall Accuracy	91.7 (55/60)	91.7 (55/60)	95 (57/60)	91.7 (55/60)
	OPTN criteria			
	Reader 1		Reader 2	
	CECT	EOB-MRI	CECT	EOB-MRI
Meeting MC	96.2 (51/53)	94.3 (50/53)	98.1 (52/53)	98.1 (52/53)
Exceeding MC	42.9 (3/7)	57.1 (4/7)	42.9 (3/7)	42.9 (3/7)
Overall Accuracy	90 (54/60)	90 (54/60)	91.7 (55/60)	91.7 (55/60)

Data are percentages, with numerators and denominators in parentheses

CECT contrast-enhanced computed tomography, *EOB-MRI* Gadoxetic acid-enhanced MRI, *LI-RADS* Liver Imaging Reporting and Data System, *MC* Milan criteria, *OPTN* Organ Procurement and Transplantation Network

significant differences between EC-MRI and EOB-MRI, particularly for lesions measuring 1–1.9 cm, although EOB-MRI outperformed EC-MRI for per-patient HCC detection.

Evaluation of whole-liver explant parenchyma has the merit of detecting HCC invisible on imaging, thereby getting truer imaging sensitivity estimates. The 'real world' or true sensitivities of EOB-MRI and CECT in LR-4/5 categories were lower in our study when analyses included all HCC diagnosed at explant histopathology irrespective of a corresponding imaging observation. A prior meta-analysis and a recent study have reported lower sensitivities of EOB-MRI in studies wherein liver explant was the only reference standard [15, 26] in line with our comparable lower real-world sensitivities with EOB-MRI. Nevertheless, in a 'real-world' scenario, EOB-MRI was significantly superior to CECT in the LR-4/5 category.

HBP signal as an AF for adjusting LI-RADS category significantly improved EOB-MRI sensitivity in LR-4/5 observations in this study, regardless of size and for < 2 cm group, without significant impact on specificity. A prior retrospective study reported no significant differences between CECT and EOB-MRI for HCC diagnosis with LR-4/5 and LR-5 categories [23]. However, AFs were only utilized to assign LR-1 or 2 categories which could have lowered EOB-MRI results. In the LR-5 category, we found an overall insignificantly higher sensitivity for CECT over EOB-MRI with a similar PPV of 100% on both imaging modalities, in alignment with their results. Although LI-RADSv2018 can be utilized for interpretation with hepatobiliary contrast agents (HBAs), unlike with extracellular contrast agents, only portal venous phase hypointensity qualifies as the washout appearance. This has implications for HCC diagnosis in the LR-5 category [26–28], probably contributing to lowered diagnostic performance of EOB-MRI in the < 2 cm HCC subgroup in our study, like few previous studies [29–31]. Although HBP hypointensity is not intended to upgrade to LR-5, it can improve HCC detection sensitivity without impairing specificity with EOB-MRI [32], as depicted by our results in the LR-4/5 category.

In our study, EOB-MRI was superior to CECT for detection of < 2 cm viable HCC in treated lesions as per LI-RADS TRA. However, without size consideration, there were no significant differences between the two modalities like in some prior studies [33, 34]. A prior study by Bae et al. [35] reported higher sensitivity of HBA-enhanced MRI over CECT. This discrepancy could be attributable to a greater percentage of conventional TACE–treated lesions in their study (73.4%) impacting accurate assessment of APHE with CECT [36]. Arterial phase subtraction images, through better visualization of APHE, have been reported to improve the sensitivity of EOB-MRI in detection of viable HCC after LRT [37] and is routinely performed in all EOB-MRI at our institution.

In this study, EOB-MRI and CECT had equivalent performances for assessing simulated LT eligibility based on MC with LI-RADSv2018 and OPTN criteria in reference to explant histopathology, even as lower accuracies were observed in prediction of patients exceeding MC. Although recent studies have demonstrated moderate to high accuracy for determining LT eligibility based on MC using CECT and EOB-MRI with LI-RADSv2018 and OPTN, however in these retrospective studies [25, 38], patients with LRT for HCC before LT were excluded. Since both non-treated and viable HCC in treated observations require to be considered for MC before LT, our study results convey more real-world accuracies. We observed a higher accuracy for identifying unsuitable LT candidates based on MC with LI-RADS versus OPTN, although statistically insignificant. Contrary to our results, a lower accuracy of LI-RADSv2018 (57.9%) vs OPTN (85.7%) has been reported in this scenario previously [38]. This difference could again be due to the exclusion of patients with treated lesions from that study. Even though classic HCC features and threshold growth criteria for definite HCC by LI-RADS (LR-5) and OPTN (OPTN-5) are similar in both systems, there are some important differences [5, 18, 39]. While OPTN criteria do not incorporate HBP features, our results support using EOB-MRI for OPTN classification, given the high accuracy obtained for LT eligibility.

We must acknowledge some limitations of this study. This was a single-center study with a limited patient cohort; however, all patients were enrolled prospectively, and explant histopathology correlation was

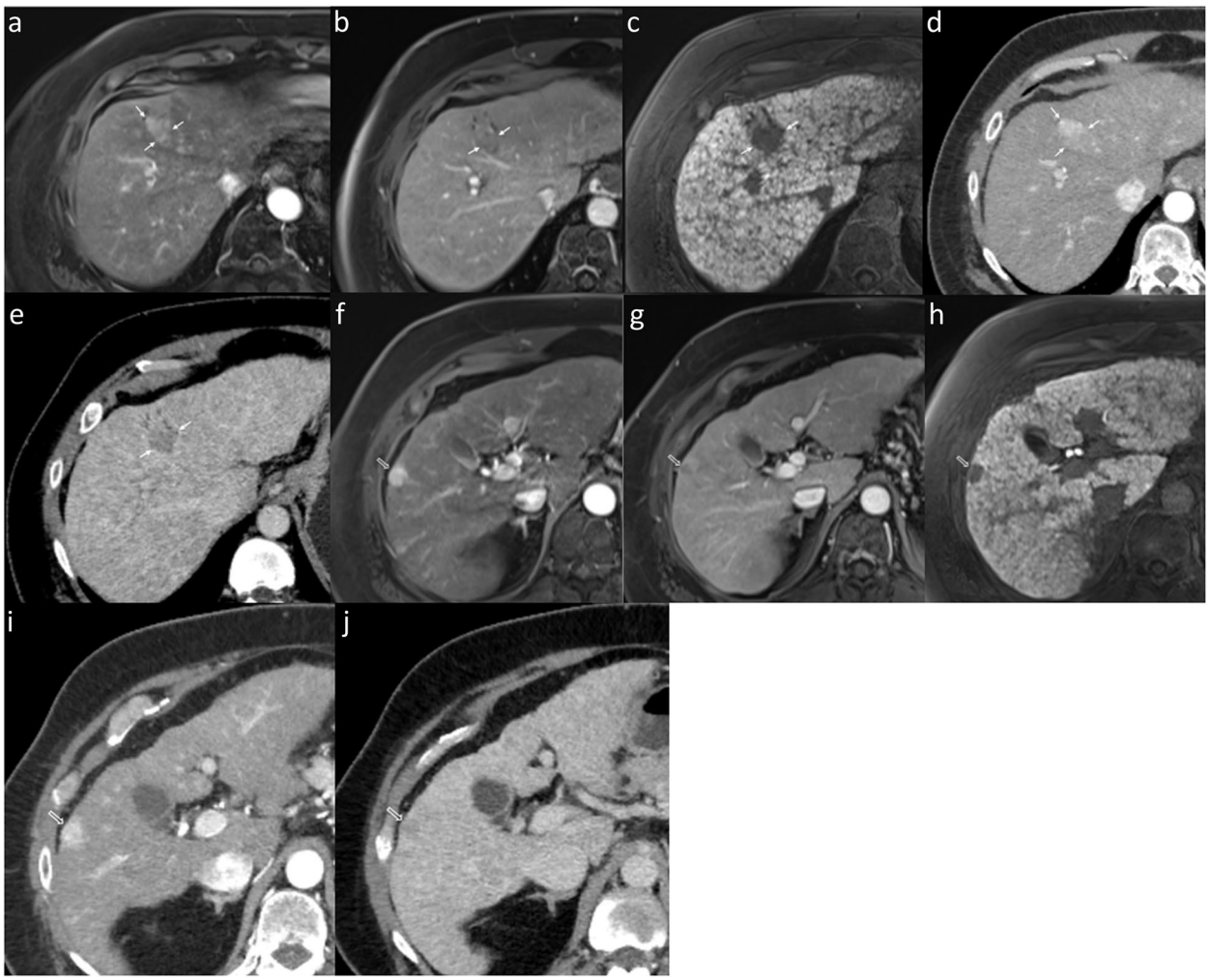

Fig. 5 Discordance in LT eligibility as per MC from HCC diagnosis by OPTN criteria and LI-RADS. In a 62-year-old man, EOB-MRI (**a**–**c**) and CECT (**d** and **e**) demonstrated a 28-mm observation with non-rim APHE (arrows, **d**) and washout (arrows, **b** and **e**), but without enhancing capsule in segment 4a/8. The lesion was categorized/classified as LR-5 and 5B by LI-RADS and OPTN criteria, respectively. Additionally, there were four 1–1.9 cm-sized LR-5 observations (one is shown in segment 5; hollow arrow, **f**–**j**), with non-rim APHE (**f** and **i**) and washout (**g** and **j**) but no enhancing capsule. Lesions demonstrated HBP hypointensity (arrows, **c**; hollow arrow, **h**). None of these five observations were eligible to be classified as 5A according to OPTN criteria due to lack of delayed peripheral enhancement, and therefore, based on the presence of a single 5B observation, the patient would be deemed as meeting the MC. In contrast, he would be considered beyond the MC according to LI-RADS categories (presence of five LR-5 observations). Since histopathologic examination of the liver explant revealed five HCC, the patient was indeed beyond MC and unsuitable for liver transplantation. Abbreviations: APHE: arterial phase enhancement, CECT: contrast-enhanced computed tomography, EOB-MRI: Gadoxetate-enhanced-MRI, HCC: hepatocellular carcinoma, HBP: hepatobiliary phase, LI-RADS: Liver Imaging Reporting and Data System, MC: Milan criteria, OPTN: Organ Procurement and Transplantation Network

available for the entire study cohort. The lack of using threshold growth in this study for assignment of LI-RADS categories may have underestimated the sensitivity for HCC diagnosis but is applicable to both modalities. The mean time interval between CECT and LT was 1 month longer than the time between EOB-MRI and LT, which could have led to changes in HCC characteristics, thereby impacting imaging evaluation variably between CECT and EOB-MRI. We acknowledge that the three-month interval may change tumor size for aggressive HCC, and it would be ideal to have both CECT and EOB-MRI performed closely before LT. However, since we could not predict the exact time-point of LT, it was not feasible to perform both EOB-MRI and CECT at every 3-month follow-up interval. It can be challenging to precisely match every lesion recorded on imaging to the liver explant, particularly with small lesion size and because of the shrinkage effects of formalin fixation. Lastly, since we used CPN or non-CPN at histopathologic examination as the

reference standard for viable HCC in treated lesions, microscopically viable HCC could have led to underestimation of LR-TR viable category.

Conclusions

EOB-MRI has superior diagnostic performance for HCC diagnosis in pre-LT cirrhotic patients over CECT in specific categories, while it was inferior to CECT for LR-5 observations less than 2 cm. While both EOB-MRI and CECT have a lower diagnostic performance in a real-world scenario, EOB-MRI outperforms CECT therein. At a patient level, LT eligibility assessment appears to be comparable between EOB-MRI and CECT; however, both modalities have relatively lower accuracies for identifying patients exceeding MC compared to those within MC.

Abbreviations

APHE	Arterial phase hyperenhancement
CPN	Complete pathologic necrosis
CECT	Contrast-enhanced Computed tomography
DWI	Diffusion-weighted imaging
EC-MRI	Extracellular gadolinium-based contrast-enhanced MRI
EOB-MRI	Gadoxetic acid-enhanced MRI
ETC	Extended Toronto criteria
FP	False positive
HCC	Hepatocellular carcinoma
HBP	Hepatobiliary phase
LI-RADS	Liver imaging reporting and data system
LI-RADS	Treatment response algorithm (LI-RADS TRA)
LT	Liver transplantation
MC	Milan criteria
MELD	Model for end-stage liver disease
NPV	Negative predictive value
OPTN	Organ Procurement and Transplantation Network
PPV	Positive predictive value
TACE	Transarterial chemoembolization
UNOS	United network for organ sharing

Supplementary Information

The online version contains supplementary material available at https://doi.org/10.1186/s40644-023-00532-3.

Additional file 1. Multiphasic Liver CT protocol (Aquilion 64).

Additional file 2. MRI Protocol for Gadoxetic acid-enhanced liver MRI (EOB-MRI).

Additional file 3. LI-RADS v2018 – Major and Ancillary Features with EOB-MRI.

Additional file 4. Lesion characteristics evaluated on EOB-MRI.

Additional file 5. Lesion characteristics evaluated on Contrast-enhanced CT scan.

Additional file 6. CECT and EOB-MRI treatment response categories.

Additional file 7. OPTN classification system for lesions seen on imaging of cirrhotic livers.

Additional file 8. Distribution of non-treated hepatocellular carcinoma (HCC) and viable HCC in explants.

Additional file 9. Histopathology results for LR-2 and LR-3 lesions scored by readers on EOB-MRI and CECT.

Acknowledgements
The study received grant funding from Bayer Canada.

Authors' contributions
KJ made substantial contributions to conception, design of work, and interpretation of data and have substantially revised the manuscript. ABJ made a substantial contribution to the data acquisition and interpretation and drafting and revising the manuscript. RB contributed to data acquisition. KE contributed to data acquisition. OE performed the statistical analysis and contributed to revising the manuscript. SF performed the histological examination of the explants. AG contributed to interpretation of data and revising the manuscript. GS contributed to interpretation of data and revising the manuscript. All authors read and approved the final manuscript.

Funding
This study received a research grant/funding support by Bayer Canada Inc.

Availability of data and materials
The datasets used and/or analysed during the current study are available from the corresponding author on reasonable request.

Declarations

Ethics approval and consent to participate
Institutional Review Board approval was obtained. Written informed consent was obtained from all subjects (patients) in this study.

Consent for publication
Not applicable.

Competing interests
The authors declare that they have no competing interests.

Author details
[1]Joint Department of Medical Imaging, University Health Network, Mount Sinai Hospital and Women's College Hospital, University of Toronto, 610 University Ave, 3-957, Toronto, ON M5G 2M9, Canada. [2]Joint Department of Medical Imaging, University Health Network, Mount Sinai Hospital and Women's College Hospital, Toronto, ON M5G 1X6, Canada. [3]Joint Department of Medical Imaging, University Health Network, Mount Sinai Hospital and Women's College Hospital, University of Toronto, Toronto, ON M5G 2M9, Canada. [4]Department of Biostatistics, Princess Margaret Cancer Centre, University Health Network, Toronto, ON M5G 2C1, Canada. [5]Division of Biostatistics, Dalla Lana School of Public Health, University of Toronto, Toronto, Canada. [6]Department of Pathology, University Health Network and University of Toronto, Toronto, Ontario, Canada. [7]University Health Network, Department of Surgery, Toronto General Hospital, University of Toronto, Toronto, ON M5G 2N2, Canada.

Received: 4 October 2022 Accepted: 8 February 2023
Published online: 25 February 2023

References

1. Llovet JM, Villanueva A, Marrero JA, Schwartz M, Meyer T, Galle PR, et al. Trial design and endpoints in hepatocellular carcinoma: AASLD consensus conference. Hepatology. 2021;73:158–91.
2. European Association for the Study of the Liver. EASL clinical practice guidelines: management of hepatocellular carcinoma. J Hepatol. 2018;69(1):182–236.
3. Filgueira NA. Hepatocellular carcinoma recurrence after liver transplantation: risk factors, screening and clinical presentation. World J Hepatol. 2019;11(3):261–72.
4. Wald C, Russo MW, Heimbach JK, Hussain HK, Pomfret EA, Bruix J. New OPTN/UNOS policy for liver transplant allocation: standardization of liver imaging, diagnosis, classification, and reporting of hepatocellular carcinoma. Radiology. 2013;266:376–82.
5. Organ Procurement and Transplant Network (OPTN) Policies https://optn.transplant.hrsa.gov/media/eavh5bf3/optn_policies.pdf. Accessed 13 Mar 2022.

6. Libbrecht L, Bielen D, Verslype C, Vanbeckevoort D, Pirenne J, Nevens F, et al. Focal lesions in cirrhotic explant livers: pathological evaluation and accuracy of pretransplantation imaging examinations. Liver Transpl. 2002;8:749–61.
7. Rode A, Bancel B, Douek P, Chevallier M, Vilgrain V, Picaud G, et al. Small nodule detection in cirrhotic livers: evaluation with US, spiral CT, and MRI and correlation with pathologic examination of explanted liver. J Comput Assist Tomogr. 2001;25:327–36.
8. Teefey SA, Hildeboldt CC, Dehdashti F, Siegel BA, Peters MG, Heiken JP, et al. Detection of primary hepatic malignancy in liver transplant candidates: prospective comparison of CT, MR imaging, US, and PET. Radiology. 2003;226:533–42.
9. de Lédinghen V, Laharie D, Lecesne R, Le Bail B, Winnock M, Bernard PH, et al. Detection of nodules in liver cirrhosis: spiral computed tomography or magnetic resonance imaging? A prospective study of 88 nodules in 34 patients. Eur J Gastroenterol Hepatol. 2002;14:159–65.
10. Roberts LR, Sirlin CB, Zaiem F, Almasri J, Prokop LJ, Heimbach JK, et al. Imaging for the diagnosis of hepatocellular carcinoma: a systematic review and meta-analysis. Hepatology. 2018;67:401–21.
11. Choi JY, Lee JM, Sirlin CB. CT and MR imaging diagnosis and staging of hepatocellular carcinoma: part II. Extracellular agents, hepatobiliary agents, and ancillary imaging features. Radiology. 2014;273:30–50.
12. Min JH, Kim JM, Kim YK, Cha DI, Kang TW, Kim H, et al. Magnetic resonance imaging with extracellular contrast detects hepatocellular carcinoma with greater accuracy than with Gadoxetic acid or computed tomography. Clin Gastroenterol Hepatol. 2020;18:2091–2100.e7.
13. Semaan S, Vietti Violi N, Lewis S, Chatterji M, Song C, Besa C, et al. Hepatocellular carcinoma detection in liver cirrhosis: diagnostic performance of contrast-enhanced CT vs. MRI with extracellular contrast vs. gadoxetic acid. Eur Radiol. 2020;30:1020–30.
14. Kakihara D, Nishie A, Harada N, Shirabe K, Tajima T, Asayama Y, et al. Performance of gadoxetic acid-enhanced MRI for detecting hepatocellular carcinoma in recipients of living-related-liver-transplantation: comparison with dynamic multidetector row computed tomography and angiography-assisted computed tomography. J Magn Reson Imaging. 2014;40:1112–20.
15. Guo J, Seo Y, Ren S, Hong S, Lee D, Kim S, et al. Diagnostic performance of contrast-enhanced multidetector computed tomography and gadoxetic acid disodium-enhanced magnetic resonance imaging in detecting hepatocellular carcinoma: direct comparison and a meta-analysis. Abdom Radiol (NY). 2016;41:1960–72.
16. Taouli B, Krinsky GA. Diagnostic imaging of hepatocellular carcinoma in patients with cirrhosis before liver transplantation. Liver Transpl. 2006;12(11 Suppl 2):S1–7.
17. Liu X, Jiang H, Chen J, Zhou Y, Huang Z, Song B. Gadoxetic acid disodium-enhanced magnetic resonance imaging outperformed multidetector computed tomography in diagnosing small hepatocellular carcinoma: a meta-analysis. Liver Transpl. 2017;23:1505–18.
18. American College of Radiology. Liver imaging reporting and data system. Available via https://www.acr.org/Clinical-Resources/Reporting-and-Data-Systems/LI-RADS. Accessed 09 Mar 2022.
19. Amin MB, Greene FL, Edge SB, Compton CC, Gershenwald JE, Brookland RK, et al. The eighth edition AJCC Cancer staging manual: continuing to build a bridge from a population-based to a more "personalized" approach to cancer staging. CA Cancer J Clin. 2017;67:93–9.
20. Sapisochin G, Goldaracena N, Laurence JM, Dib M, Barbas A, Ghanekar A, et al. The extended Toronto criteria for liver transplantation in patients with hepatocellular carcinoma: a prospective validation study. Hepatology. 2016;64:2077–88.
21. Mazzaferro V, Bhoori S, Sposito C, Bongini M, Langer M, Miceli R, et al. Milan criteria in liver transplantation for hepatocellular carcinoma: an evidence-based analysis of 15 years of experience. Liver Transpl. 2011;17(Suppl 2):S44–57.
22. Sternberg MR, Hadgu A. A GEE approach to estimating sensitivity and specificity and coverage properties of the confidence intervals. Stat Med. 2001;20(9-10):1529–39.
23. Nakao S, Tanabe M, Okada M, Furukawa M, Iida E, Miyoshi K, et al. Liver imaging reporting and data system (LI-RADS) v2018: comparison between computed tomography and gadoxetic acid-enhanced magnetic resonance imaging. Jpn J Radiol. 2019;37:651–9.
24. Lee SM, Lee JM, Ahn SJ, Kang HJ, Yang HK, Yoon JH. LI-RADS version 2017 versus version 2018: diagnosis of hepatocellular carcinoma on Gadoxetate disodium-enhanced MRI. Radiology. 2019;292:655–63.
25. Bae JS, Lee DH, Lee SM, Suh KS, Lee KW, Yi NJ, et al. Performance of LI-RADS version 2018 on CT for determining eligibility for liver transplant according to Milan criteria in patients at high risk for hepatocellular carcinoma. AJR Am J Roentgenol. 2022;219(1):86–96.
26. Clarke CGD, Albazaz R, Smith CR. Comparison of LI-RADS with other noninvasive liver MRI criteria and radiological opinion for diagnosing hepatocellular carcinoma in cirrhotic livers using gadoxetic acid with histopathological explant correlation. Clin Radiol. 2021;76:333–41.
27. Hope TA, Fowler KJ, Sirlin CB. Hepatobiliary agents and their role in LI-RADS. Abdom Imaging. 2015;40:613–25.
28. Zech CJ, Ba-Ssalamah A, Berg T. Consensus report from the 8th international forum for liver magnetic resonance imaging. Eur Radiol. 2020;30:370–82.
29. Song JS, Choi EJ, Hwang SB, Hwang HP, Choi H. LI-RADS v2014 categorization of hepatocellular carcinoma: Intraindividual comparison between gadopentetate dimeglumine-enhanced MRI and gadoxetic acid-enhanced MRI. Eur Radiol. 2019;29:401–10.
30. Tang A, Bashir MR, Corwin MT, LI-RADS Evidence Working Group. Evidence supporting LI-RADS major features for CT- and MR imaging-based diagnosis of hepatocellular carcinoma: a systematic review. Radiology. 2018;286:29–48.
31. Joo I, Lee JM, Lee DH, Ahn SJ, Lee ES, Han JK. Liver imaging reporting and data system v2014 categorization of hepatocellular carcinoma on gadoxetic acid-enhanced MRI: comparison with multiphasic multidetector computed tomography. J Magn Reson Imaging. 2017;45:731–40.
32. Lee S, Kim SS, Bae H, Shin J, Yoon JK, Kim MJ. Application of liver imaging reporting and data system version 2018 ancillary features to upgrade from LR-4 to LR-5 on gadoxetic acid-enhanced MRI. Eur Radiol. 2021;31:855–63.
33. Seo N, Kim MS, Park MS, Choi JY, Do RKG, Han K, et al. Evaluation of treatment response in hepatocellular carcinoma in the explanted liver with liver imaging reporting and data system version 2017. Eur Radiol. 2020;30:261–71.
34. Park S, Joo I, Lee DH. Diagnostic performance of LI-RADS treatment response algorithm for hepatocellular carcinoma: adding ancillary features to MRI compared with enhancement patterns at CT and MRI. Radiology. 2020;296:554–61.
35. Bae JS, Lee JM, Yoon JH. Evaluation of LI-RADS version 2018 treatment response algorithm for hepatocellular carcinoma in liver transplant candidates: Intraindividual comparison between CT and hepatobiliary agent-enhanced MRI. Radiology. 2021;299:336–45.
36. Kloeckner R, Otto G, Biesterfeld S, Oberholzer K, Dueber C, Pitton MB. MDCT versus MRI assessment of tumor response after transarterial chemoembolization for the treatment of hepatocellular carcinoma. Cardiovasc Intervent Radiol. 2010;33:532–40.
37. Youn SY, Kim DH, Choi JI. Usefulness of arterial subtraction in applying liver imaging reporting and data system (LI-RADS) treatment response algorithm to Gadoxetic acid-enhanced MRI. Korean J Radiol. 2021;22:1289–99.
38. Jeon SK, Lee JM, Joo I, Yoo J, Park JY. Comparison of guidelines for diagnosis of hepatocellular carcinoma using gadoxetic acid-enhanced MRI in transplantation candidates. Eur Radiol. 2020;30:4762–71.
39. Cunha GM, Tamayo-Murillo DE, Fowler KJ. LI-RADS and transplantation: challenges and controversies. Abdom Radiol (NY). 2021;46:29–42.

Publisher's Note